

# Competition between anion binding and dimerization modulates *Staphylococcus aureus* phosphatidylinositol-specific phospholipase C enzymatic activity

Authors: Jiongjia Cheng, Rebecca Goldstein, B. Stec, A. Gershenson, Mary F. Roberts

Persistent link: <http://hdl.handle.net/2345/bc-ir:107107>

This work is posted on [eScholarship@BC](#),  
Boston College University Libraries.

---

Published in *Journal of Biological Chemistry*, vol. 287, no. 48, pp. 40317-40327, 2012

© the American Society for Biochemistry and Molecular Biology. These materials are made available for use in research, teaching and private study, pursuant to U.S. Copyright Law. The user must assume full responsibility for any use of the materials, including but not limited to, infringement of copyright and publication rights of reproduced materials. Any materials used for academic research or otherwise should be fully credited with the source.

# Competition between Anion Binding and Dimerization Modulates *Staphylococcus aureus* Phosphatidylinositol-specific Phospholipase C Enzymatic Activity<sup>\*[5]</sup>

Received for publication, June 30, 2012, and in revised form, October 3, 2012. Published, JBC Papers in Press, October 4, 2012, DOI 10.1074/jbc.M112.395277

Jiongjia Cheng<sup>‡</sup>, Rebecca Goldstein<sup>‡</sup>, Boguslaw Stec<sup>§</sup>, Anne Gershenson<sup>¶</sup>, and Mary F. Roberts<sup>‡1</sup>

From the <sup>‡</sup>Department of Chemistry, Boston College, Chestnut Hill, Massachusetts 02467, the <sup>§</sup>Sanford-Burnham Medical Research Institute, La Jolla, California 92037, and the <sup>¶</sup>Department of Biochemistry and Molecular Biology, University of Massachusetts, Amherst, Massachusetts 01003

**Background:** Bacterial phosphatidylinositol-specific phospholipase C targets PI and glycosylphosphatidylinositol-linked proteins of eukaryotic cells.

**Results:** Functional relevance of a homodimeric *S. aureus* PI-PLC crystal structure is supported by enzyme kinetics and mutagenesis. Nonsubstrate phosphatidylcholine increases activity by facilitating enzyme dimerization.

**Conclusion:** Activating transient dimerization is antagonized by anions binding to a discrete site.

**Significance:** Interplay of protein oligomerization and anion binding controls enzyme activity.

*Staphylococcus aureus* phosphatidylinositol-specific phospholipase C (PI-PLC) is a secreted virulence factor for this pathogenic bacterium. A novel crystal structure shows that this PI-PLC can form a dimer via helix B, a structural feature present in all secreted, bacterial PI-PLCs that is important for membrane binding. Despite the small size of this interface, it is critical for optimal enzyme activity. Kinetic evidence, increased enzyme specific activity with increasing enzyme concentration, supports a mechanism where the PI-PLC dimerization is enhanced in membranes containing phosphatidylcholine (PC). Mutagenesis of key residues confirm that the zwitterionic phospholipid acts not by specific binding to the protein, but rather by reducing anionic lipid interactions with a cationic pocket on the surface of the *S. aureus* enzyme that stabilizes monomeric protein. Despite its structural and sequence similarity to PI-PLCs from other Gram-positive pathogenic bacteria, *S. aureus* PI-PLC appears to have a unique mechanism where enzyme activity is modulated by competition between binding of soluble anions or anionic lipids to the cationic sensor and transient dimerization on the membrane.

Secreted bacterial phosphatidylinositol-specific phospholipase C (PI-PLC)<sup>2</sup> enzymes contribute to virulence in pathogenic bacteria. These enzymes catalyze the cleavage of PI or glycan phosphatidylinositol-anchored proteins to diacylglycerol and an inositol 1,2-(cyclic)-phosphate. Several of these enzymes are kinetically activated by the zwitterionic phospho-

lipid phosphatidylcholine (PC) (1–3). Intriguingly, the activation mechanism varies among the PI-PLCs. *Bacillus* PI-PLC enzymes exhibit high affinity for PC interfaces and specifically bind at least one PC molecule quite tightly (4). The enzyme from *Listeria monocytogenes* is activated by many amphiphiles in a somewhat nonspecific fashion where the diluting lipid prevents protein-induced vesicle aggregation and the resulting sequestration of the enzyme. This nonspecific activation mechanism also likely reduces penetration of the highly cationic protein into a negatively charged bilayer (3). Consistent with this mode of PC activation, *L. monocytogenes* PI-PLC has very low affinity for PC small unilamellar vesicles (SUVs) but very high affinity for anionic phospholipid interfaces.

*Staphylococcus aureus* PI-PLC, a likely virulence factor whose production was shown to be up-regulated in a study of methicillin-resistance *S. aureus* (5), presents yet another wrinkle in the properties of these exoproteins. Its optimum activity is around pH 6.5, and unlike the other homologues it is strongly inhibited by moderate concentrations of salt (6, 7). A recent structure of the protein (7) showed two features not found in other PI-PLCs: (i) a  $\pi$ -cation latch, which appears important for water-soluble product release at low pH where the protein is tightly bound to vesicle surfaces, and (ii) a surface anion-binding pocket distinct from the active site that could explain the salt sensitivity. *S. aureus* PI-PLC activity is also enhanced by the presence of PC in assays systems (7).

We have solved a novel crystal structure of *S. aureus* PI-PLC, formed in the presence of dibutyryl-PC, with significant intermonomer contacts at the interface of the hydrophobic side chains of helix B and no anion in the anion binding pocket. This is strikingly different from previous, monomeric crystal structures (7). The relevance of this dimer structure to protein function and regulation has been tested by measuring enzymatic activity and lipid binding of recombinant enzyme and variants with selected mutations. The experimental findings suggest that *S. aureus* PI-PLC is optimally active as a dimer when, as the crystal structure suggests, the anion binding pocket is occluded.

\* This work was supported, by National Institutes of Health Grant R01 GM60418 (to M. F. R.).

[5] This article contains supplemental Figs. S1 and S2.

<sup>1</sup> To whom correspondence should be addressed. Tel.: 617-552-3616; Fax: 617-552-2705; E-mail: mary.roberts@bc.edu.

<sup>2</sup> The abbreviations used are: PI-PLC, phosphatidylinositol-specific phospholipase C; cIP, inositol 1,2-(cyclic)phosphate; dIC<sub>4</sub>PC, 1,2-dibutyryl-*sn*-glycero-3-phosphocholine; FCS, fluorescence correlation spectroscopy; PC, 1-palmitoyl-2-oleoylphosphatidylcholine; PG, 1,2-dioleoyl-*sn*-glycero-3-phospho-(1'-*rac*-glycerol); PI, L- $\alpha$ -phosphatidylinositol; SUV, small unilamellar vesicle; WT, wild type recombinant *S. aureus* PI-PLC; X<sub>PC</sub>, mole fraction PC.

## Dimerization of *S. aureus* PI-PLC on Target Membranes

PC activates the enzyme by diluting anionic substrate (which has some affinity for the anion binding pocket as well as the active site), enhancing transient PI-PLC aromatic side chain  $\pi$ /choline cation interactions, and in turn allowing transient dimers to form. This complex mechanism, in which electrostatic interactions, spatially removed from the active site, compete with dimerization facilitated by zwitterionic PC, may be a broadly applicable mechanism allowing differential regulation of peripheral membrane enzymes by specific phospholipids.

### EXPERIMENTAL PROCEDURES

**Chemicals**—L- $\alpha$ -Phosphatidylinositol and other phospholipids, including 1,2-dibutyroyl-*sn*-glycero-3-phosphocholine (diC<sub>4</sub>PC), PC, and 1,2-dioleoyl-*sn*-glycero-3-phospho-(1'-rac-glycerol) (PG), were purchased from Avanti Polar Lipids, Inc., and used without further purification. All competent cells used in mutagenesis (XL1-Blue) and overexpression (BL21 Codonplus) were obtained from Stratagene. LB media and LB agar were obtained from Fisher Scientific, Inc. The fluorescent dye Alexa Fluor 488 carboxylic acid, succinimidyl ester was purchased from Invitrogen. Nickel-nitrilotriacetic acid-agarose resin was purchased from Qiagen and Q-Sepharose fast-flow anion-exchange resin was purchased from GE Healthcare. Bio-Spin 6 columns were obtained from Bio-Rad Laboratories. All other chemicals were purchased from Sigma.

**PI-PLC Enzymes**—Recombinant *S. aureus* PI-PLC was produced and purified as described previously (7). Mutations in the *piplc* gene were made using site-directed mutagenesis (Stratagene) and complementary primers purchased from Operon to generate the PI-PLC variants V44C, V44W, H86E, H86Y, F249W, Y253K, Y253S, Y253W, Y290A, and Y253S/Y255S. The sequence of each mutated gene was confirmed by Genewiz. *Escherichia coli* BL21-Codonplus (DE3)-RIL cells were transformed with the plasmid containing the *S. aureus piplc* gene. Overexpression and purification of the His-tagged recombinant protein followed protocols reported previously (7). The purity of the PI-PLC enzymes was above 95% as monitored by SDS-PAGE; concentrations were measured by the absorption at 280 nm using  $\epsilon_{280} = 60,280 \text{ M}^{-1} \text{ cm}^{-1}$  calculated by ProtParam (8). Secondary structure and thermal stability of *S. aureus* PI-PLC variants were determined using far-UV CD as described previously for *Bacillus thuringiensis* PI-PLC (9). Compared with recombinant wild type *S. aureus* PI-PLC (WT), there are no significant changes in structure and thermal stability for the single mutation enzymes. Although Y253S/Y255S has the same secondary structure content, its thermal denaturation temperature is 5 °C lower than WT. Recombinant *B. thuringiensis* PI-PLC was generated as described previously (9).

**Crystallography**—Purified *S. aureus* PI-PLC was concentrated to 20 mg/ml before being combined with 100 mM myo-inositol and, in the case of WT only, 5 mM diC<sub>4</sub>PC. Each mixture was diluted to a final concentration of 10 mg/ml using deionized water. The protein was incubated on ice for a minimum of 2 h before setting up crystallization trays. Samples were crystallized at 20 °C by vapor diffusion, using hanging drops of 3  $\mu$ l. Crystals of the recombinant PI-PLC were obtained in 150 mM ammonium acetate, 100 mM sodium acetate, pH 4.6, with 1 mM Mg(NO<sub>3</sub>)<sub>2</sub>, and 20% PEG 4000. Except for the presence of

the monomeric diC<sub>4</sub>PC, these conditions differ from those used previously (7) only in the inclusion of Mg(NO<sub>3</sub>)<sub>2</sub>. Y253S crystals were obtained using similar conditions with an increase in the concentration of Mg(NO<sub>3</sub>)<sub>2</sub> to 100 mM, and a slight decrease in PEG 4000 (to 16%). WT *S. aureus* PI-PLC crystals appeared as large plates and formed in the drop after approximately nine months, whereas the Y253S crystals appeared as plates after 2 weeks. Suitable crystals were mounted in nylon loops and frozen in liquid nitrogen.

Data were collected at 100 K using an in-house Rigaku MicroMax-07 HF high intensity microfocus rotating Cu anode x-ray generator, coupled with Osmic VariMax Optics and a R-Axis IV++ image plate area detector. Data were indexed and reduced using HKL2000 (10). Both the dimer, and the Y253S mutant structures were solved by molecular replacement using PHASER in CCP4 (11, 12) with *S. aureus* PI-PLC structure 3V16 (7) as a model. The models were refined using Refmac (12) with manual model building in COOT (13). Ligands and ligand restraints were generated using the PRODRG2 server (14). Structural comparisons were made using SSM superposition (15) in COOT and alignment in PyMOL (Schrodinger). ProCheck (16) was used for structure validation and Adit (17) was used for deposition.

**Preparation of Phospholipid Aggregates**—Enzyme kinetics experiments used PI/PC small unilamellar vesicles (SUVs) prepared by sonication, where  $X_{\text{PC}}$  is the mole fraction of PC in these SUVs. Aliquots of phospholipids (PI, PG, and PC species) in chloroform were mixed, dried under N<sub>2</sub>, and then lyophilized overnight. The lipid film was rehydrated with the desired buffer. Small PI/PC vesicles were generated by sonicating lipid mixtures for 10 to 15 min on ice (Branson Sonifier 250). The average radii for PI and PI/PC ( $X_{\text{PC}} = 0.5$ ) vesicles were 130 Å, with 20 and 46% polydispersity, respectively. Similar sizes have also been documented for the PG/PC SUVs used in FCS experiments (18).

**<sup>31</sup>P NMR Assays of PI-PLC Activity**—Specific activities of the PI-PLC enzymes were measured by monitoring production of cIP from PI by <sup>31</sup>P NMR spectroscopy (Varian VNMRS 600) (1, 2, 9). Most assays were in 50 mM MES, pH 6.5, with 1 mM EDTA and 0.1 mg/ml of bovine serum albumin at 28 °C. However, for assays examining the pH dependence of activity, a mixed buffer system of MES and HEPES (total concentration of 50 mM) with the required pH value was used. Specific activities in the presence of salt were determined using a NaCl (137 mM)/KCl (2.7 mM) mixture. *S. aureus* PI-PLC concentrations used in assays ranged from 0.2 to 8  $\mu$ g/ml. The enzyme and SUVs were incubated for fixed times at 28 °C, and the reaction was quenched by addition of acetic acid followed by Triton X-100 to solubilize the remaining lipids in mixed micelles. The relative integrated intensity of the cIP resonance versus the total phospholipid concentration was used to calculate PI-PLC specific activity. For all reactions, the cleavage of PI was kept below 20% (no inositol 1-phosphate was generated under these conditions). The increase in cIP under these conditions is linear with time indicative of an initial rate being measured. Because we are dealing with a vesicle and some fusion of SUVs as diacylglycerol is produced, this is not the same as a steady-state rate with the substrate in solution, but it is operationally useful for compar-

ing rates under different conditions (pH, concentration of enzyme, salt, etc.).

*S. aureus* PI-PLC Vesicle Binding Measured by Fluorescence Correlation Spectroscopy (FCS)—*S. aureus* PI-PLC proteins were labeled at pH 7.2 to maximize preferential labeling of the N terminus with Alexa Fluor 488 succinimidyl ester according to the manufacturer's protocol (Invitrogen). After removal of unbound dye using 3 spin columns, the absorption at 280 nm for protein plus dye and at 495 nm for the dye were used to estimate the number of dye molecules incorporated. Labeled *S. aureus* PI-PLC typically had 93–100% dye incorporation. Electrospray ionization mass spectral data of intact PI-PLC were obtained at the University of Massachusetts Amherst Mass Spectrometry Facility, which is supported in part by the National Science Foundation. Labeling percentages ranged from 80 to 99% with >70% of the protein containing a single Alexa Fluor 488 moiety and the remainder doubly labeled. At 99% labeling efficiency, 25–30% of the labeled protein has 2 labels, whereas this percentage is lower (20–25%) at 80% labeling. The activity of labeled PI-PLC is not significantly different from that of unlabeled PI-PLC.

FCS-based binding assays were performed on a home-built confocal setup described previously (18, 19). The fluorescence was monitored at 22 °C with samples placed in chambered coverglass wells (Lab-Tek, Nunc), containing 10 nM labeled PI-PLC and 1 mg/ml of bovine serum albumin in 300  $\mu$ l of 50 mM MES buffer, pH 6.5 (the same buffer used in the enzymatic assays). The anionic phospholipid PG was used as the substrate analog. For vesicle binding experiments, Alexa Fluor 488-labeled PI-PLC variants were titrated with unlabeled PG/PC vesicles, where  $X_{PC}$  was varied between 0 and 1. For each  $X_{PC}$ , FCS titrations were run in duplicate and repeated a second time with different vesicle and protein preparations. Data analysis was based on previous work by Elson, Thompson and others (20–24) and similar to that described for *B. thuringiensis* PI-PLC (25). The fitted diffusion coefficient for free, Alexa Fluor 488-labeled *S. aureus* PI-PLC ( $D_{free}$ ) was  $50 \pm 2 \mu\text{m}^2 \text{s}^{-1}$  and the vesicle diffusion coefficient,  $D_{bound}$ , determined from analysis of vesicles containing fluorescently labeled lipids, was in the range of 12–15  $\mu\text{m}^2 \text{s}^{-1}$  (18, 19). To account for the possibility that multiple proteins could bind to the same vesicle, autocorrelations ( $G(\tau)$ ) (obtained in cross-correlation mode using a 50–50 beamsplitter) for samples containing SUVs were fit to Equation 1 (22–24),

$$G(\tau) = A_p g_p(\tau) + A_v g_v(\tau) \quad (\text{Eq. 1})$$

where  $p$  and  $v$  denote free protein and SUVs that are fluorescent due to PI-PLC binding, respectively, and  $A_j$  is the amplitude of species  $j$ . The correlation function for species  $j$ ,  $g_j(\tau)$  is shown in Equations 2–4 (20–22),

$$g_j(\tau) = \left(1 + \frac{\tau}{\tau_{D,j}}\right)^{-1} \left(1 + \frac{\tau}{S^2 \tau_{D,j}}\right)^{-1/2} \quad (\text{Eq. 2})$$

$$\tau_{D,j} = \frac{\omega_0^2}{4D_j} \quad (\text{Eq. 3})$$

$$S = \frac{z_0}{\omega_0} \quad (\text{Eq. 4})$$

where the values of  $\omega_0$ , the radius of the observation volume in the  $x$  and  $y$  directions, and  $S$ , which depends on  $z_0$ , the extent of the observation volume, were determined from fits to the rhodamine 110 calibration data using  $D = 280 \text{ nm}^2 \text{ s}^{-1}$  at 22 °C (21).  $\tau_{D,j}$  is the diffusion time. The fraction of protein bound to the SUVs,  $f$ , is determined from  $A_p$  and the time-averaged number of proteins in the observation volume,  $\langle N_o \rangle$ , as described previously (18). The average brightness of the SUVs relative to the protein (22, 24),  $\alpha = A_v / (A_{po} - A_p)$ , where  $A_{po}$  is the correlation amplitude in the absence of vesicles, had values around 1 for *S. aureus* PI-PLC, again indicating that for PI-PLC and these small PG/PC vesicles, on average one protein is bound per SUV during the diffusion time of  $\sim 190$  ms.

The apparent dissociation constant,  $K_d$ , representing PI-PLC partitioning to the vesicle surface, and a cooperativity coefficient,  $n$ , was determined using the empirical equation (18, 19),

$$f = f_{max} [PL]^n / (K_d^n + [PL]^n) \quad (\text{Eq. 5})$$

where  $f$ , the fraction of protein bound to the vesicles, is determined for different total lipid concentrations,  $[PL]$ , at fixed  $X_{PC}$ , and  $f_{max}$  is the apparent maximum fraction bound. Although fits to Equation 1 assume that all of the SUVs have the same diffusion coefficient, the SUVs are polydisperse with a rather broad size (18). This assumption does not cause the apparent  $K_d$  values to significantly deviate from the actual values, but does result in values for  $f_{max}$  that are less than one, even for computer-generated data where  $f_{max} = 1$ .

## RESULTS

*S. aureus* PI-PLC Dimer Structure—Previously reported crystal structures of *S. aureus* PI-PLC show a monomeric protein with significantly different, pH-dependent conformations of a rim loop near the active site (7) and the structure of the basic form is very similar to that of the *Bacillus* PI-PLCs (25, 26). However, in the presence of diC<sub>4</sub>PC and Mg(NO<sub>3</sub>)<sub>2</sub> at pH 4.6, we serendipitously found that the protein crystallized as a complete homodimer in the asymmetric unit (Fig. 1). This protein crystallizes in a variety of unit cells with very different crystal packing (supplemental Fig. S1). However, this particular crystal structure is the only one to date where the dimer is not the result of crystal contacts. This new crystal form was in the P2<sub>1</sub> space group, with unit cell  $a = 43.36 \text{ \AA}$ ,  $b = 133.38 \text{ \AA}$ ,  $c = 50.19 \text{ \AA}$ ,  $\beta = 89.95^\circ$ . The dataset was twinned and was found to have the twinning operator of  $H, -K, -L$  with a fraction of 45.1%. Using twinned refinement in Refmac we have successfully improved the  $R$  values from the untwinned refinement ( $R_{cryst} = 0.261$ ,  $R_{free} = 0.322$ ) to the final twinned refinement ( $R_{cryst} = 0.215$  and  $R_{free} = 0.250$ ). No distinct density consistent with diC<sub>4</sub>PC was observed. Crystallization as a dimer in the presence of diC<sub>4</sub>PC might be indicative of an additional control mechanism at the membrane surface.

In the dimer, both monomers have their mobile loops in the compact, acidic-like conformation with Phe-249 forming an intramolecular  $\pi$ -cation interaction with His-258, which pulls

## Dimerization of *S. aureus* PI-PLC on Target Membranes

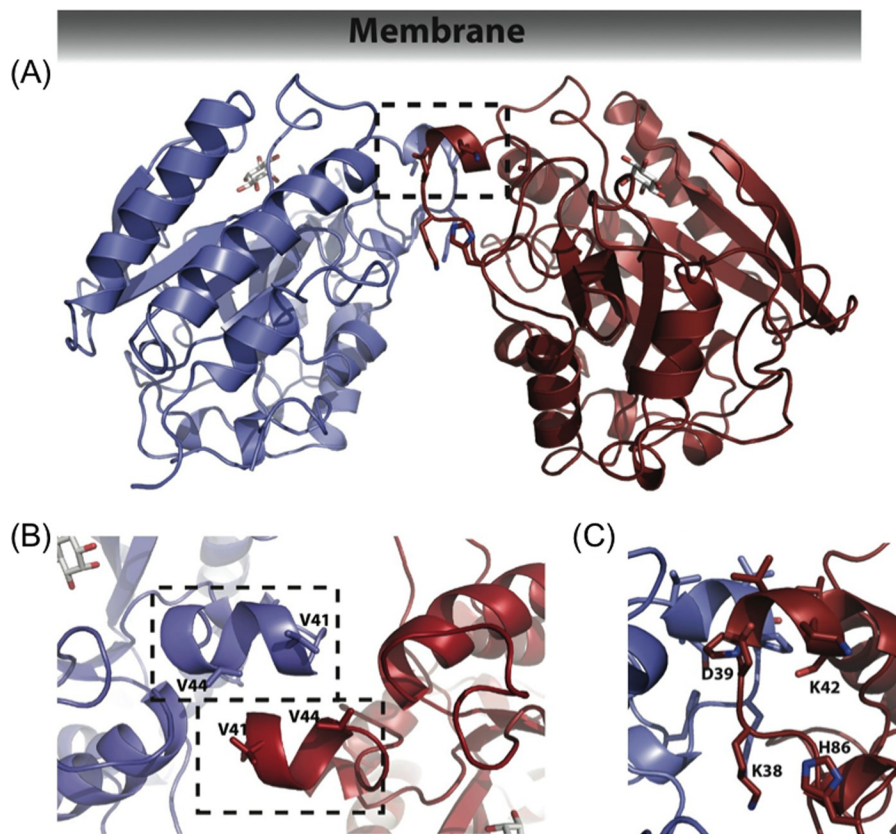


FIGURE 1. *S. aureus* PI-PLC can form a homodimer. *A*, *S. aureus* PI-PLC dimer structure, crystallized at pH 4.6 with the addition of 100 mM *myo*-inositol and 5 mM  $\text{diC}_4\text{PC}$ , with *B*, a close-up of the dimer interface. In *A*, residues that coordinate an anion in monomer structures are shown to indicate their relationship to the dimer interface. *C*, close up view of the anion binding site with key residues labeled.

the mobile loop in line with the barrel rim. Each monomer contains one molecule of *myo*-inositol in the active site, and the monomers are oriented in a head to head fashion with respect to each other (Fig. 1*A*). The dimer interface is formed by the direct interaction of the side chains belonging to helix B of each monomer (Fig. 1*B*). The area of contact is quite small (primarily consisting of residues 38–44 and adjacent regions, including residues 50, 250–254, 282, and 285, with a total buried surface area of 565.7 Å<sup>2</sup>, or 4.7% of the total surface area), and held together primarily by hydrophobic interactions, with only 6 hydrogen bonds between the two monomers. Each monomer only gains 3.9 kcal/mol upon complex formation (as evaluated with the PISA service), which would suggest a very transient dimer in solution (27). The main inter-monomer contact is the alignment of Val-41 from one monomer with Val-44 from the opposite monomer to form a hydrophobic box. When viewed as a dimer, an area of hydrophobicity can clearly be seen at the interface (Fig. 1, *B* and *C*), as well as along the barrel rim. Besides contributing to dimer formation, the valine box could also directly participate in membrane binding. Several other interactions aid the valine box in holding the monomers together. An ionic bond forms between Lys-38 and Asp-50 from the opposing monomer, and a hydrogen bond occurs between the backbone carbonyl of Thr-36 and the side chain hydroxyl of Tyr-285 from the opposing monomer. This helical valine box, along with several hydrophobic side chains, would orient the active site toward the membrane.

The anion binding pocket adjacent to helix B in the *S. aureus* PI-PLC monomer structure is made up of the backbone amides of Asp-38 and Lys-39, as well as the cationic side chains of His-86 and Lys-42 (7). This open surface pocket is shaped to snugly fit a tetrahedral anion such as phosphate or sulfate. Anionic phospholipid could also localize in the vicinity of this cationic site. However, in the dimer, helix B of one monomer occludes the pocket of the other (Fig. 2*B*), limiting water-soluble or membrane-bound anion binding. Thus, in the dimer, this unoccupied positively charged region could contribute to electrostatic steering to anionic phospholipids, but the binding pocket is no longer accessible.

Although the secondary structures of both *Bacillus* and *Listeria* proteins are quite similar to that of *S. aureus* PI-PLC, kinetic evidence suggests that those other proteins do not function as dimers. As will be shown in Fig. 4, the specific activity of *B. thuringiensis* PI-PLC does not increase with increasing protein concentration (and previous work showed that the enzyme was a monomer in solution (1)). The *L. monocytogenes* PI-PLC specific activity decreased with increasing protein concentration strongly suggesting it does not function as a dimer (3). Examining crystal structures for each of those would suggest that if they do form transient dimers on a membrane, it is not with the helix B orientation found in the crystal structure for that protein (supplemental Fig. S2). Significant conformational changes in this region would be needed.

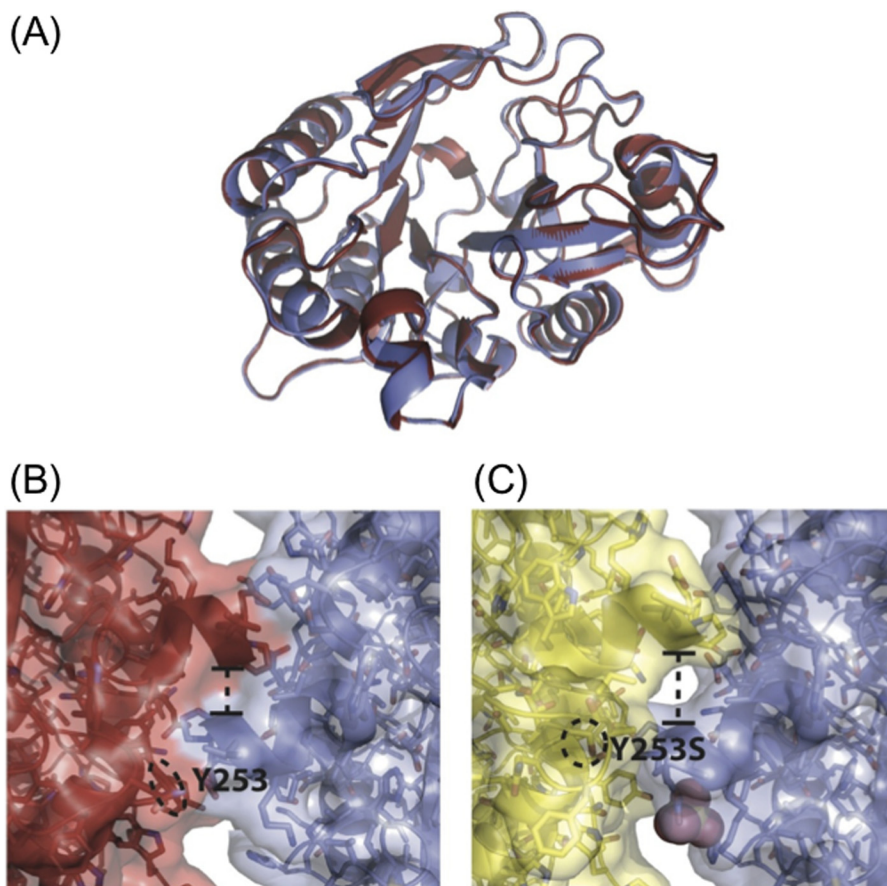


FIGURE 2. **Anion binding destabilizes the dimer interface.** *A*, overlay of monomers A and B from the WT dimer. The backbone structure between the two monomers is very similar. View of the anion binding pocket as seen looking down from the membrane interface in *B*, the homodimer, where it is unoccupied, and *C*, the *in silico* Y253S dimer, generated from the monomer with a sulfate ion bound in the anion site. In both *B* and *C* a dashed circle indicates the side chain of residue 253. With an anion bound in the pocket, the distance between the two monomers (indicated by the dashed line, measured from the  $\alpha$  carbon of Val-41) widens, destabilizing the dimer interface.

Although crystallographically elegant, it is unclear whether the *S. aureus* PI-PLC dimer structure is functionally relevant. If the dimer is the active form of PI-PLC, PI-PLC cleavage of PI in small unilamellar vesicles in the absence and presence of PC should display the following characteristics. (i) Specific activity should increase with increasing enzyme concentration in a saturable manner. (ii) If PC kinetic activation functions to enhance dimer formation, then the dependence of specific activity on enzyme concentration should shift to lower protein concentrations. (iii) If formation of the dimer and occupation of the nearby anion binding pocket are mutually exclusive, the enzyme should show reduced sensitivity to soluble anions under conditions that favor dimerization.

***S. aureus* PI-PLC Enzymatic Activity: Testing for a Functional Oligomer**—The pH optimum for *S. aureus* PI-PLC enzymatic activity depends on the SUV composition (7). Toward pure PI SUVs, the pH optimum is pH 5.5–6, whereas for vesicles with 0.5  $X_{PC}$ , the optimum is shifted to pH 6.5–7 (Fig. 3A). Thus, most assays were carried out at pH 6.5. Specific activity increases dramatically when PC is present in the bilayer (Fig. 3B). Similar PC enhanced activity and a shift in the pH profile were observed with PI dispersed in micelles of diheptanoyl-PC versus Triton X-100 (Fig. 3C). Unlike *B. thuringiensis* PI-PLC, where specific activity decreases when  $X_{PC} > 0.5$  (18), no sur-

face dilution inhibition is observed for *S. aureus* PI-PLC with increasing PC content up to 0.8  $X_{PC}$ , either for fixed total phospholipid (as shown in Fig. 3B) or fixed PI with increasing amounts of PC. Because the dimer structure with its occluded anion binding site was obtained in the presence of PC, *S. aureus* PI-PLC salt sensitivity might be ameliorated by PC. Indeed, the presence of PC rescues the loss of activity observed at moderate salt concentrations (Fig. 3B), and higher  $X_{PC}$  results in lower salt sensitivity. This is consistent with a transient dimer that has lost the ability to bind soluble anions in the anion binding pocket. That this is an interfacial phenomenon is shown by cIP kinetics (Fig. 3D), which exhibit both only a small activation by diheptanoyl-PC micelles and only about a 2-fold drop in specific activity with added salt.

A more direct indication of a functional dimer is the observation that, in the absence of salt, *S. aureus* PI-PLC specific activity is dependent on enzyme concentration, particularly when the substrate is pure PI SUVs (Fig. 4A). For comparison, the specific activity of *B. thuringiensis* PI-PLC, which is unlikely to form the same dimer through helix B, does not depend on enzyme concentration and is only weakly salt dependent (Fig. 4B). If PC is present in the bilayer, there is still an increase in *S. aureus* PI-PLC-specific activity with increasing enzyme concentration, but this reaches an optimal value at a much lower

## Dimerization of *S. aureus* PI-PLC on Target Membranes

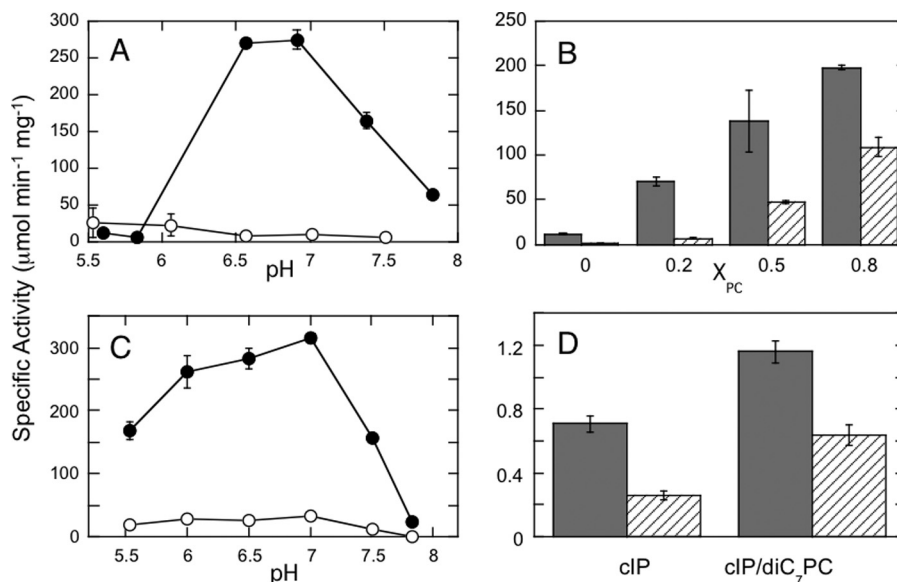


FIGURE 3. PC modulates the pH and salt dependence of *S. aureus* PI-PLC activity as measured by production of cIP from PI using  $^{31}\text{P}$  NMR. *A*, the pH dependence for *S. aureus* PI-PLC cleavage of PI in pure PI SUVs (4 mM) (○) and PI/PC (4 mM/4 mM) (●) SUVs. *B*, specific activity at pH 6.5 increases with increasing  $X_{\text{PC}}$  and is not as sensitive to the addition of 140 mM salt. Filled bars, no salt; hatched bars, plus 140 mM salt. The total phospholipid concentration was held constant at 4 mM for the indicated  $X_{\text{PC}}$ . The enzyme concentration was 4  $\mu\text{g}/\text{ml}$  for pure PI SUVs and 0.3  $\mu\text{g}/\text{ml}$  for PI/PC SUVs. *C*, specific activity for cleavage of 4 mM PI in 8 mM Triton X-100 (○) or 16 mM diheptanoyl-PC (●) micelles. *D*, specific activity toward 5 mM cIP alone or with 5 mM diheptanoyl-PC and in the absence (grey column) or presence of 140 mM salt (hatched). Error bars in each plot represent S.D. from multiple assays.

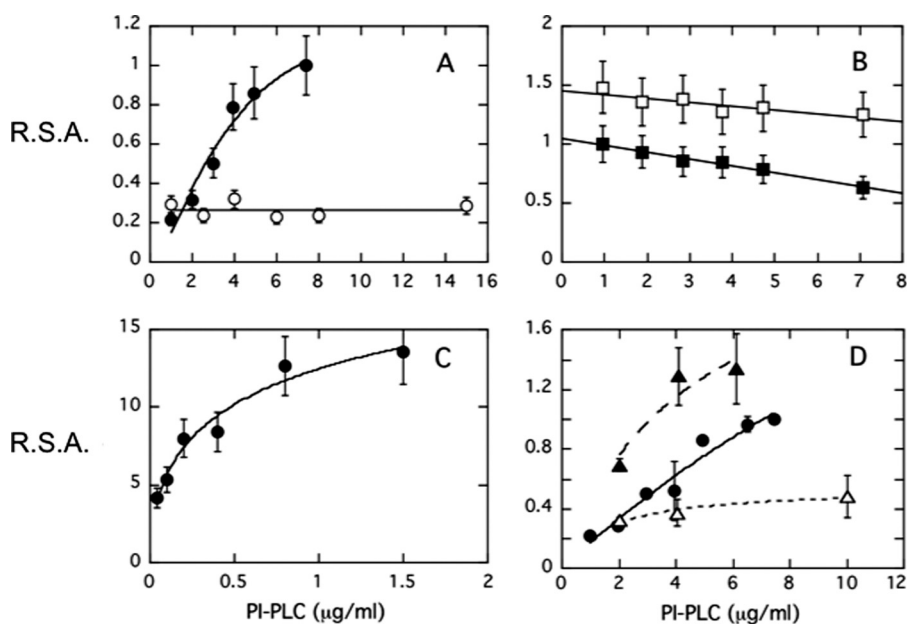


FIGURE 4. *S. aureus* PI-PLC relative specific activity (R.S.A.), as measured by production of cIP from PI using  $^{31}\text{P}$  NMR, increases with enzyme concentration suggesting oligomerization of this protein (but not *B. thuringiensis* PI-PLC) on interfaces. For *S. aureus* PI-PLC, specific activities are normalized to the highest specific activity obtained for WT enzyme acting on 4 mM PI SUVs in the absence of added salt (9.8  $\mu\text{mol min}^{-1} \text{mg}^{-1}$  at pH 6.5). For *B. thuringiensis* PI-PLC activities are normalized to 164  $\mu\text{mol min}^{-1} \text{mg}^{-1}$  at pH 7.5, the optimal activity toward 8 mM PI SUVs in the absence of salt. R.S.A. as a function of protein concentration is shown for: *A*, *S. aureus* PI-PLC toward PI (4 mM) SUVs in the absence (●) and presence (○) of 140 mM salt; *B*, *B. thuringiensis* PI-PLC toward 8 mM PI SUVs in the absence (■) and presence (□) of 140 mM salt; *C*, *S. aureus* PI-PLC activity toward PI (8 mM)/PC (8 mM) SUVs in the absence of salt; and *D*, V44C (△) and V44W (▲) compared with the WT *S. aureus* PI-PLC (●) toward 4 mM PI SUVs.

enzyme concentration (Fig. 4C). This dependence of PI-PLC-specific activity on protein concentration *strongly* suggests that the optimally active form of the enzyme is a dimer. The presence of PC in the membrane must shift the equilibrium between protein monomer and oligomer to lower protein concentrations.

As a further test of this hypothesis we mutated Val-44, one of the key components of the dimer interface in the crystal struc-

ture. This valine was replaced with: (i) a cysteine, a small amino acid capable of hydrogen bonding that is likely to destabilize the dimer interface (a large excess of DTT was present to prevent any disulfide formation) or (ii) a tryptophan, a large side chain with a propensity to partition into membranes that might be expected to strengthen the transient dimer interaction. For PI SUVs, the specific activity of V44C was lower than that of the WT enzyme and increased at most 2-fold (compared with

5-fold for WT) over the protein concentration range examined (Fig. 4D). In contrast, the specific activity of V44W was higher than wild type and appeared to reach a maximum value at lower enzyme concentrations. These data clearly indicate that *S. aureus* PI-PLC functions optimally as a transient dimer on the SUVs. They strongly suggest that enhanced protein dimerization on the surface is part of the PC activation mechanism for *S. aureus* PI-PLC.

**The Effect of PC on *S. aureus* PI-PLC Vesicle Binding**—For *B. thuringiensis* PI-PLC, increasing  $X_{PC}$  up to 0.8 also increases the affinity of the enzyme for SUVs, and tight binding ( $K_d < 10 \mu\text{M}$ ) sequesters the enzyme on the vesicles inhibiting enzyme activity (19). *S. aureus* PI-PLC behaves quite differently. As shown in Fig. 5A, *S. aureus* PI-PLC binds well, with mM  $K_d$  values, to either PG or PG/PC (1:1) SUVs at acidic pH, but binding at pH 7.5 is much weaker, indicating that the primary interaction is electrostatic. At pH 6.5, where optimal activity is observed, the enzyme has high affinity for anionic phospholipid-rich bilayers ( $X_{PC} \leq 0.5$ ), with fairly low affinity for PC-rich bilayers (Fig. 5B). Indeed, binding to pure PC SUVs could not be measured. The apparent  $K_d$  for pure PG vesicles is  $0.38 \pm 0.14 \text{ mM}$  at pH 6.5, and this value corresponds well with the apparent  $K_m$  value ( $0.23 \pm 0.03 \text{ mM}$ ) for cleavage of PI in pure PI SUVs (Fig. 5C). For  $X_{PC} = 0.5$ , again the apparent  $K_d$  determined by FCS ( $2.5 \pm 0.5 \text{ mM}$ ) is approximately the same as the kinetic apparent  $K_m$  for PI/PC SUVs ( $1.9 \pm 0.5 \text{ mM}$ ). *S. aureus* PI-PLC apparent  $K_d$  values increase with PC content and the enzyme binds much less tightly at high PC. For these compositions, and in the absence of salt, the  $K_m$  reflects the  $K_d$  for vesicle binding as measured by FCS.

Added salt reduces the affinity for PG-rich SUVs to such an extent that the apparent  $K_d$  for pure PG SUVs could not be measured. To explore this further we examined the fraction of protein bound to a large excess of vesicles (18 mM PG) in the absence and presence of NaCl (Fig. 5A, inset). Without salt, all of the protein partitioned onto the vesicles, whereas increasing the ionic strength dramatically reduced protein binding. With  $\sim 130 \text{ mM}$  NaCl, only  $\sim 20\%$  of the protein was bound. Given the high bulk phospholipid concentration (18 mM), in the presence of salt the apparent  $K_d$  for PG vesicles must be very high ( $>50 \text{ mM}$ ). This result suggests that *S. aureus* PI-PLC binding to pure PG vesicles is almost entirely mediated by electrostatic interactions. However, with PC in the vesicle, the much higher residual activity indicates that binding of the enzyme to the bilayer now has a more substantial hydrophobic component.

**Perturbing Hydrophobic Interactions with the Membrane**—In the *Bacillus* enzymes, a number of aromatic residues are critical for tight binding to PC-rich membranes, including Trp-242, which partitions into the bilayer (9, 25), and a strip of four surface Tyr residues in helix G (26). In *S. aureus* PI-PLC, Trp-242 is replaced by Phe-249 and this enzyme has only two of the four tyrosine residues (Tyr-253 and Tyr-255) in helix G. It is also unclear if Phe-249 interacts with the membrane because it is tucked into the protein and away from the surface in the monomeric acidic *S. aureus* PI-PLC crystal structure (7) and in the dimer structure described here. To test whether these residues interact with the membrane in *S. aureus* PI-PLC, we constructed the following variants: F249W and F249I, Y253S, and

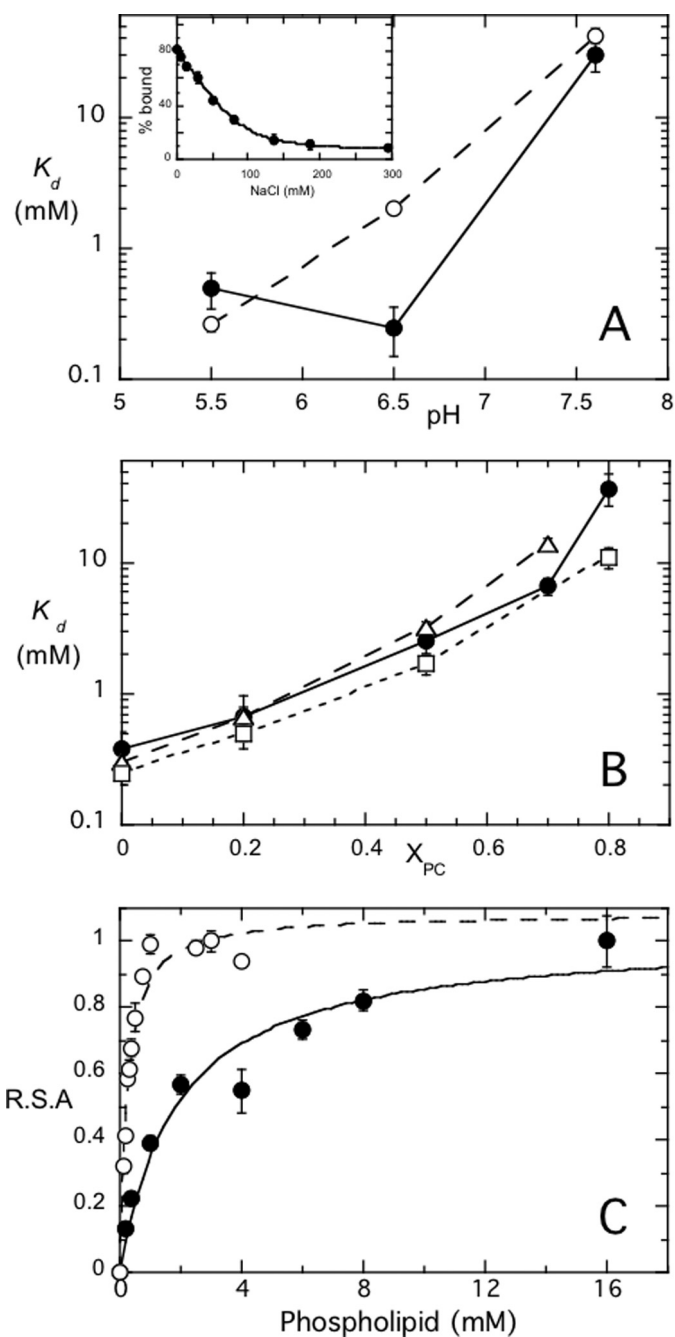


**FIGURE 5. *S. aureus* PI-PLC binding affinity, measured by FCS, increases with pH and PC content and is similar to the apparent  $K_m$  for the enzyme.** Variation of the PI-PLC apparent dissociation constant,  $K_d$ , for SUVs as a function of: A, pH for PG (●) and PG/PC ( $X_{PC} = 0.5$ ) (○), and B, mole fraction PC,  $X_{PC}$ , at pH 6.5, for WT (●), F249W (□), and Y253S/Y255S (Δ). The inset in A shows the fraction of WT protein bound to pure PG (18 mM) SUVs at pH 6.5 as the concentration of salt is increased. C, relative specific activity of *S. aureus* PI-PLC as a function of total phospholipid concentration ([PI] + [PC]) at  $X_{PC} = 0$  (○) and 0.5 (●) at pH 6.5. The amount of enzyme used was  $0.1 \mu\text{g/ml}$  for pure PI SUVs and  $0.2 \mu\text{g/ml}$  for experiments with PI/PC SUVs. For each system the observed activity was normalized to the maximum observed activity,  $11.2 \mu\text{mol min}^{-1} \text{mg}^{-1}$  for pure PI SUVs and  $282 \mu\text{mol min}^{-1} \text{mg}^{-1}$  for the PI/PC SUVs. The error bars are the S.D. from independent experiments.

Y253S/Y255S. Tyr-290, a single Tyr residue that is unlikely to interact with the membrane, was also mutated to serine as a control. As shown in Fig. 6, the activity of the control, Y290S, is similar to WT. However, both Y253S and the double Tyr mutant enzyme are much less active under all conditions.

## Dimerization of *S. aureus* PI-PLC on Target Membranes

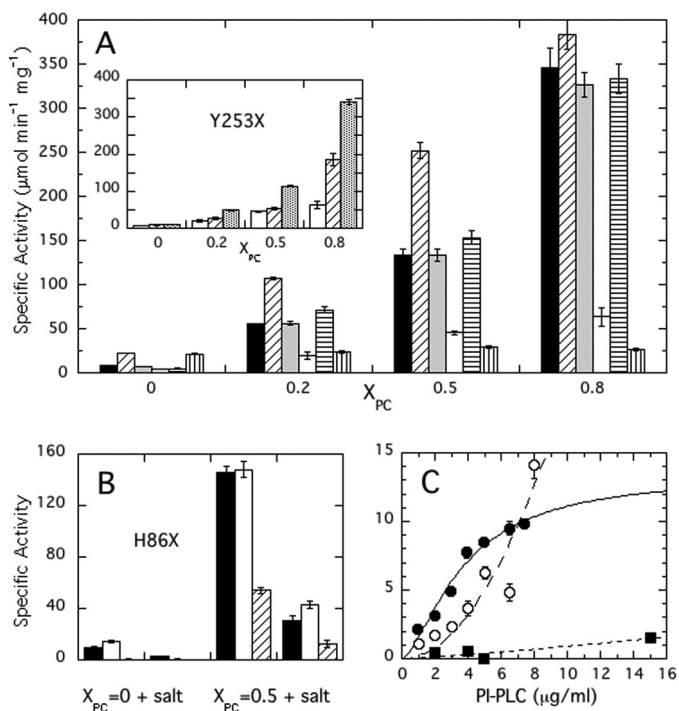


**FIGURE 6. Specific activities of *S. aureus* PI-PLC variants as a function of  $X_{PC}$  at pH 6.5.** *A*, WT (■), F249W (▨), F249I (grey column), Y253S (□), Y290S (▤), and Y253S/Y255S (▥). The inset shows the activity of Y253 variants: Y253S (□), Y253K (▨), and Y253W (▤). *B*, specific activities for H86 variants toward pure PI SUVs and PI/PC (1:1) SUVs in the absence and presence of added salt: H86Y (□) and H86E (▨) are compared with WT (■). The kinetic experiments in *A* and *B* kept the PI concentration at 4 mM and increased the PC to yield the indicated  $X_{PC}$ . *C*, dependence of PI-PLC specific activity on protein concentration: WT (●), H86Y (○), and H86E (■). Error bars are the S.D. of activities measured in triplicate.

Increasing PC content has a very modest effect on PI cleavage by Y253S, whereas Y253S/Y255S is virtually insensitive to the presence of PC. In contrast, mutating Phe-249 to a tryptophan significantly enhanced enzyme activity for  $X_{PC} \leq 0.5$ , whereas the activity of F249I is equivalent to that of the WT. The pH dependence was varied for several of these variants, and whereas F249I and Y290S still behave essentially like WT, Y253S exhibits much lower activity regardless of pH (data not shown). The loss of activity and PC activation for Y253S and Y253S/Y255S suggest that these residues play a role in the conformational change(s) that activate the protein in the presence of PC.

Because both F249W and Y253S/Y255S have activities that are significantly different from WT, protein binding to PG/PC SUVs was measured by FCS (Fig. 5B). The  $K_d$  values for F249W are comparable with WT at  $X_{PC} = 0$  and 0.2 but significantly smaller at 0.8  $X_{PC}$ , indicative of enhanced interactions with the membrane as might be expected when the larger tryptophan side chain replaces a phenylalanine that inserts into the membrane. However, this higher affinity for PC-rich SUVs does not translate into significantly higher activity. For comparison, Y253S/Y255S has similar affinities to WT up to 0.7  $X_{PC}$ , but much lower activity. For higher PC content, the fraction of mutant protein bound was small and linear up to 50 mM phospholipid, and the apparent  $K_d$  could not be estimated. These surface tyrosine residues are important for PC enhancement of activity; however, except at 0.8  $X_{PC}$ , the loss of activity is not a

**TABLE 1**

**Crystallographic summary for the *S. aureus* PI-PLC dimer and for monomeric Y253S**

Protein	WT dimer	Y253S
<b>PDB ID</b>	4F2B	4F2T
<b>Diffraction data</b>		
Resolution range (Å)	66.7–2.16	29.89–2.30
Reflections	27,485	13,541
Reflections in free set	1,534	678
Space group	P2 <sub>1</sub>	P2 <sub>1</sub> ,2 <sub>1</sub> ,2 <sub>1</sub>
Unit cell		
a (Å)	43.36	86.1
b (Å)	133.38	55.96
c (Å)	50.19	61.68
$\beta$ (°)	89.95	90
Monomers in the A.U.	2	1
Completeness	95.4	98.4
$R_{merge}$	0.063	0.063
<b>Refinement</b>		
$R_{cryst}$ <sup>a</sup>	0.215	0.187
$R_{free}$	0.250	0.241
Residues	606	302
Non-H protein atoms	4844	2420
Non-H inositol atoms	24	0
H <sub>2</sub> O molecules	123	132
Ions	0	3
Root mean square deviation bonds (Å)	0.024	0.008
Root mean square deviation angles (Å)	2.1	1.2
<b>Ramachandran plot (%)</b>		
Most favored	85.8	90
Additionally allowed	14	9.6
Generously allowed	0.2	0.4
Disallowed	0	0
Average B-factor (Å <sup>2</sup> )	42.46	44.64

<sup>a</sup>  $R_{cryst} = \frac{\sum (||F_o| - |F_c||)}{\sum |F_o|}$ , where  $|F_o|$  and  $|F_c|$  are the observed and calculated structure factor amplitudes, respectively.

<sup>b</sup> Ref. 30.

result of reduced binding. Thus, unlike *Bacillus* PI-PLC where  $K_d$  values for SUVs vary by orders of magnitude (from micromolar to >100 mM), as a function of  $X_{PC}$  and/or enzyme mutations, the range of  $K_d$  for *S. aureus* PI-PLC is much more limited and less easily perturbed.

**Occupation of the Anion Binding Pocket versus Dimerization**—Compared with WT, Y253S has little activation by PC but similar membrane affinity. To help explain this behavior, a 2.3-Å structure of Y253S was obtained at pH 4.6. This variant crystallized as a monomer in the P2<sub>1</sub>,2<sub>1</sub>,2<sub>1</sub> space group, with a unit cell of  $a = 86.1$  Å,  $b = 55.96$  Å, and  $c = 61.68$  Å. The Y253S structure was refined down to a final  $R_{cryst}$  value of 0.187 ( $R_{free}$  of 0.241). Statistics for the structure are given in Table 1. In the homodimer structure, the  $\alpha$ -carbon of residue 253 is 14.7 Å away from the active site, and, whereas not a direct part of the anion binding pocket, Tyr-253 aids in occluding the anion-binding site. When compared with the *S. aureus* monomeric PI-PLC structures, all catalytic residues in Y253S appear unchanged. The structure is essentially identical to the WT monomeric structure at the same pH except around the mutation site. This mutation also has no effect on the acid form of the mobile rim loop. The monomer structure for Y253S, therefore, offers little explanation for the loss of PC activation in Y253S. However, when the native homodimer structure is used as a model to create an *in silico* Y253S homodimer, there is a significant perturbation in the region of the anion binding pocket, which is empty in the homodimer. Tyr-253 aids in formation of a lid for the pocket in the opposing monomer of the homodimer structure (Fig. 2B). Replacement of the Tyr side chain with a serine leaves an opening in the adjacent monomer, thus

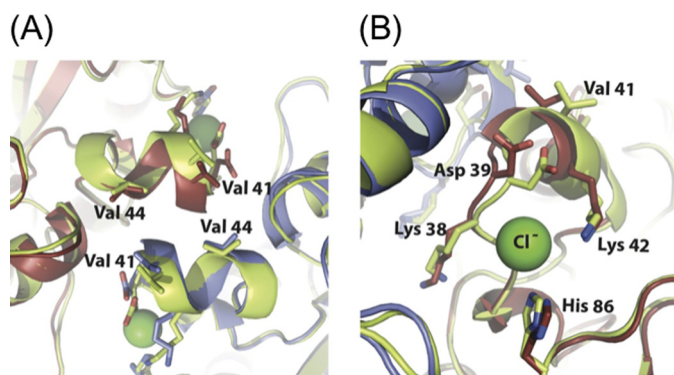


**FIGURE 7. View of the helix B dimer interface as seen looking down from the membrane interface (A), and from the side of the protein viewing the anion binding pocket (B) (the membrane surface is at the top of the two helix B moieties).** In both structures, the homodimer is seen in red and blue, whereas two green acidic monomer structures are overlaid on the dimer subunits. The homodimer has no salt bound in the anionic binding pocket, whereas the acidic monomers contain a chloride ion (green sphere).

increasing anion access to the anion binding pocket in any Y253S homodimer (Fig. 2C). This increased accessibility could facilitate soluble anion or interfacial anionic phospholipid binding to the site. Binding of ligand to the anion binding pocket in turn would destabilize the dimer interface by shifting helix B slightly away from the surface and lengthening distances between side chains that make up the tenuous dimer interface. This is visualized in Fig. 7 by comparing two monomer structures with bound chloride overlaid on the dimer. There are slight changes in the opposing helix B moieties. Helix B and the section of the adjacent loop move slightly to bind the ion. This slight shift would pull Val-41 back from the dimer interface. This separation of the valines would destabilize the already small dimer interface.

To further explore the role of the anion binding pocket and activity, two other mutant enzymes were generated: Y253W, where the “lid” for the pocket is now considerably larger, likely preventing anion binding and favoring dimerization, and Y253K, where the positive charge might increase and enhance anion binding electrostatically, although this could be balanced by the methylene chain occluding the pocket. As seen in the inset in Fig. 6A, Y253W has specific activity much higher than Y253S and comparable with WT. Y253K has lower activity than Y253W at all  $X_{PC}$  examined. However, it is not as compromised as Y253S, suggesting that the bulk of the lysine alkyl chain may be blocking access to the anion site.

As a further test of how modulating the anion binding pocket can affect activity we also prepared H86Y and H86E. The His-86 imidazole forms part of the anion binding pocket. H86Y will remove the side chain positive charge but will keep the lid in place in the dimer. H86E should antagonize anion binding because we are replacing a positive charge with a negative one. As shown in Fig. 6B, H86Y exhibits higher activity toward pure PI SUVs ( $14.1 \pm 1.0$  versus  $9.8 \pm 0.3 \mu\text{mol min}^{-1} \text{mg}^{-1}$  for WT) and activity comparable with WT with PI/PC SUVs. In contrast, H86E has very low activity toward pure PI SUVs (electrostatic repulsion would impede strong binding to SUVs), but is dramatically enhanced with PC present (a 135-fold increase compared with the more typical 10–15-fold for H86Y and WT). Consistent with the low activity toward PI SUVs, H86E

showed only a small increase in activity with enzyme concentration compared with the other proteins, reflecting its difficulty in binding to the target membrane. With  $X_{PC} = 0.5$  SUVs, the relative loss of activity for H86E in the presence of salt (29% residual activity) was also less than WT (21% residual activity). This behavior also suggests that the anion binding pocket is intertwined with dimer formation.

These results suggests a very intriguing proposal: *S. aureus* PI-PLC is optimally active as a dimer, but an appropriate phospholipid interface and/or high protein concentration is needed to at least transiently stabilize this structure. Soluble anions compete for the anion binding pocket, and prevent dimer formation as well as weakening interfacial binding. An anionic phospholipid might interact with this site, but in doing so, it would also destabilize the dimer, leading to lower activity while aiding in binding the protein to the bilayer. The observation that the double mutant Y253S/Y255S behaves similarly to Y253S supports the importance of this single aromatic group in indirectly promoting interfacial dimerization.

## DISCUSSION

*S. aureus* PI-PLC Activity, Dimer Formation, and the Membrane PC Content—The kinetic and structural data strongly suggest that *S. aureus* PI-PLC is optimally active as a dimer, and that this dimer is transiently stabilized by the membrane surface. The small dimer interface in the crystal structure suggests that dimers are likely to be transient, making them difficult to observe. *S. aureus* PI-PLC might aggregate to a small extent in solution, but obtaining accurate sizes for bacterial PI-PLCs in solution is difficult because they have an affinity for carbohydrates. At the protein concentrations required for gel filtration or analytical ultracentrifugation, these PI-PLCs interact with the resin or sucrose leading to aberrant sizes (28). Furthermore, increased ionic strength, which suppresses interaction of the *B. thuringiensis* enzyme with resins (1), would favor monomeric *S. aureus* PI-PLC. However, the simple membrane-induced dimer model does not explain why *S. aureus* PI-PLC activity increases with increasing PC content despite its lower affinity for PC-rich membranes. The presence of PC in the vesicle also rescues activity lost by the enzyme in moderate concentrations of salt (Fig. 4), consistent with a switch from electrostatic to hydrophobic interactions.

A better understanding of *S. aureus* PI-PLC might be gained by comparing it to the well studied PI-PLC from *B. thuringiensis*, which has a specific binding site for PC near helices F and G (4). For *B. thuringiensis* PI-PLC, apparent  $K_d$  values range from  $\sim 4$  mM for anionic SUVs to  $\sim 2 \mu\text{M}$  at  $X_{PC} = 0.75$  with apparent  $K_d$  values of 200–30  $\mu\text{M}$  from 0.2 to 0.5  $X_{PC}$  where enzyme activity is optimal (18). *S. aureus* PI-PLC binds more weakly to PC containing SUVs with apparent  $K_d$  values of 0.3 to  $\sim 50$  mM for 0 to 0.8  $X_{PC}$ , likely due to its lack of a PC specific binding site near the F and G helices (4, 7).

Why then does *S. aureus* PI-PLC activity increase with PC content when the affinity for vesicles is decreasing? Incorporation of PC may dilute the surface concentration of the anionic phospholipids in vesicles, and that in turn could enhance *S. aureus* PI-PLC dimer formation. This mechanism is consistent with the observation that much lower enzyme concentrations

## Dimerization of *S. aureus* PI-PLC on Target Membranes

are required to increase PI-PLC specific activity in the presence of PC (Fig. 4C) even though the apparent  $K_m$  increases as PC is increased. Alternatively, there are a number of aromatic residues in loops and N-terminal portions of helices around the barrel rim that could form transient  $\pi$ -cation interactions with the choline headgroup (7). This could alter the conformation of loops or side chains and facilitate transient protein dimerization. It should also be noted that the  $\pi$ -cation latch is still observed in the dimer structure (obtained at pH 4.6), and its presence is likely to aid in soluble cIP release, at least at acidic pH. However, the altered pH profile in the presence of PC might suggest that the zwitterionic phospholipid leads to alterations of  $pK_a$  values for the many histidine residues in and around the active site. This could be the result of a conformational change or change in the surface charge of the membrane. Additionally, interactions with PC and transient dimerization could better orient *S. aureus* PI-PLC relative to the membrane surface, facilitating enzyme activity by increasing substrate access.

**The Anion Binding Pocket, a Key to Inhibiting Dimer Formation**—One of the unusual features of *S. aureus* PI-PLC is the very electropositive anion binding pocket just below the rim of the barrel, adjacent to helix B. Neither the *Bacillus* enzymes nor *L. monocytogenes* PI-PLC have such a pocket. In *S. aureus* PI-PLC the anion pocket is composed of the backbone amides of Lys-38 and Asp-39, as well as the cationic side chains of Lys-42 and His-86. In all solved *S. aureus* PI-PLC structures (7),<sup>3</sup> except the dimer, there is electron density for an anion in this cationic pocket. Anion binding leads to a shift in the pocket residues, as well as nearby helix B. Lys-38 and Asp-39 move  $\sim 1$  Å closer to the anion, as do His-86 and Lys-42 (Fig. 7). These shifts pull the entirety of helix B (Val-41 to Ala-46) down, closer to the anion binding pocket, and thus away from the dimer interface by  $\sim 1.3$  Å. The shift in helix B residues upon salt binding to the anion binding pocket would, in turn, pull Val-41 and Val-44 farther away from the valines on the opposing monomer increasing the distance of the valine pairs from 4.5 Å in the dimer to 6.7 Å. This would weaken the hydrophobic interactions between the valine residues, destabilizing the dimer interface. The dimer interface itself is quite small consisting of only 14 residues. With an anion bound in the pocket, 10 of these residues show shifts of up to 1.5 Å, small movements, but enough to weaken the dimer interactions. Thus anion binding, probable at high salt concentrations, and dimer formation appear mutually exclusive.

**Conclusions**—We hypothesize that competition between anion binding and dimer formation is the key regulator of *S. aureus* PI-PLC activity as summarized in Fig. 8. Soluble anion binding weakens protein affinity for PI-rich vesicles, inhibiting *S. aureus* PI-PLC even at moderate salt concentrations. An anionic phospholipid might also bind to the pocket electrostatically, and thus aid in anchoring the protein to the surface. However, the presence of an anionic phospholipid such as PI near this site would favor the monomer and lead to low specific activity. High protein concentrations allow dimerization to

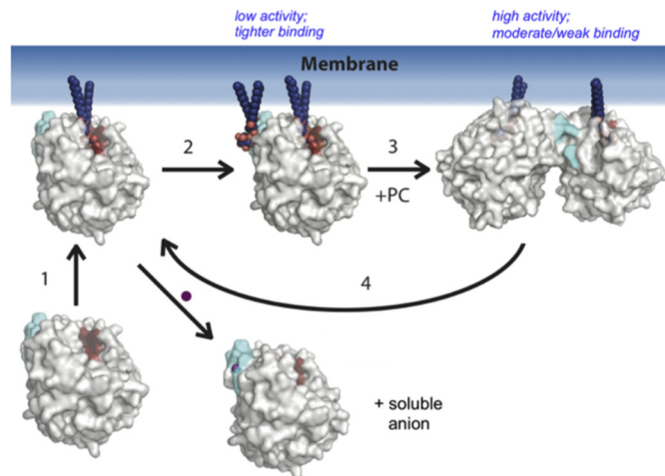


**FIGURE 8. A model for *S. aureus* PI-PLC-membrane interactions.** Monomeric PI-PLC partitions from solution to the membrane via electrostatic interactions, and a molecule of PI diffuses to the active site (step 1). The enzyme then either binds a soluble anion, and falls off the membrane, or may bind an auxiliary anionic lipid in/near the anion binding pocket (step 2). PI-PLC dimerization is promoted by PC, which dilutes the interfacial concentration of the auxiliary anionic lipid, and releases it from the enzyme (step 3). Finally, in step 4, the dimer dissociates into monomers or dissociates from the membrane. PI-PLC is represented in a semitransparent space filling view, with the active site highlighted in red, and the anion binding pocket highlighted in cyan. PI lipids are modeled as blue spheres, the membrane is shown as a blue gradient, and a water-soluble anion is shown as a purple sphere.

compete with anionic lipid binding to the pocket leading to some dimers on the membrane, but activities are still low. PC then activates *S. aureus* PI-PLC, not by specific interactions, but by lowering the interfacial anionic lipid concentration and emptying the anion binding pocket, facilitating dimer formation. Occlusion of the pocket by the dimer interface makes the membrane-bound dimer much less sensitive to physiological salt concentrations. However, there is a trade-off: dimers have higher activity, likely because of a conformational change that enhances catalysis (7) and/or because they optimize the protein orientation on the membrane for catalysis, but they bind more weakly than monomers. On PC-rich bilayers they have lost the electrostatic interactions of the regulatory site.

The association of an auxiliary anion binding site with *S. aureus* PI-PLC but not with homologues from other Gram-positive bacterial species would argue that it is related to the biology of *S. aureus*. Because abscesses are acidic (29), the slightly more acidic optimum of *S. aureus* PI-PLC enzymatic activity would make it more effective. In a study of methicillin-resistant *S. aureus*, expression of the PI-PLC, as well as other exoproteins and cytoplasmic proteins, was significantly increased (5). Although this protein has a moderate affinity for anionic surfaces in the absence of salt, once the enzyme is secreted into the moderate ionic strength of the extracellular milieu, it will not interact with other *S. aureus* organisms. It is then poised to interact with the PC or sphingomyelin-containing membranes of eukaryotic target cells via the valine box of the dimer. The still weak interaction with pure PC surfaces may allow it to hone in on negatively charged regions (the cationic character of the anion binding pocket is still available), which include GPI-anchors, the targets of this exoprotein. Clearly, this small soluble phospholipase has evolved in a complex,

<sup>3</sup> R. Goldstein, unpublished data.

apparently unique way to control its access to the phosphatidylinositol moieties that are its substrates. (i) A  $\pi$ -cation latch allows it to work on membranes under acidic conditions and more easily release soluble product without dissociating from the surface (7). (ii) An anion binding pocket near the region that binds to the membrane likely modulates the location of the protein, whether it is bound to a negatively charged surface, one with significant zwitterionic lipid content, or in solution. (iii) High activity requires dimerization of the enzyme and dimerization is enhanced by PC content similar to that found in the external leaflet of mammalian plasma membranes. This interplay between protein dimerization and an anion sensing site could be a way of regulating other peripheral (or even integral) membrane enzymes. Juxtamembrane cationic regions, whereas favoring anionic membrane regions, could prohibit protein/protein interactions. However, an appropriately modified bilayer composition might change this balance.

*Acknowledgment*—We thank Dr. Rinat Abzalimov of the University of Massachusetts Amherst Mass Spectrometry Facility for analysis of the mass spectra.

## REFERENCES

- Zhou, C., Qian, X., and Roberts M. F. (1997) Allosteric activation of phosphatidylinositol specific phospholipase C. Specific phospholipid binding anchors the enzyme to the interface. *Biochemistry* **36**, 10089–10097
- Qian, X., Zhou, C., and Roberts, M. F. (1998) Phosphatidylcholine activation of bacterial phosphatidylinositol phospholipase C toward PI vesicles. *Biochemistry* **37**, 6513–6522
- Chen, W., Goldfine, H., Ananthanarayanan, B., Cho, W., and Roberts, M. F. (2009) *Listeria monocytogenes* phosphatidylinositol-specific phospholipase C. Kinetic activation and homing in on different interfaces. *Biochemistry* **48**, 3578–3592
- Pu, M., Orr, A., Redfield, A. G., and Roberts, M. F. (2010) Defining specific lipid binding sites for a peripheral membrane protein in situ using subtesla field-cycling NMR. *J. Biol. Chem.* **285**, 26916–26922
- Burlak, C., Hammer, C. H., Robinson, M. A., Whitney, A. R., McGavin, M. J., Kreiswirth, B. N., and Deleo, F. R. (2007) Global analysis of community-associated methicillin-resistant *Staphylococcus aureus* exoproteins reveals molecules produced *in vitro* and during infection. *Cell Microbiol.* **9**, 1172–1190
- Daugherty, S., and Low, M. G. (1993) Cloning, expression and mutagenesis of phosphatidylinositol-specific phospholipase C from *Staphylococcus aureus*. A potential staphylococcal virulence factor. *Infect. Immun.* **61**, 5078–5089
- Goldstein, R., Cheng, J., Stec, B., and Roberts, M. F. (2012) Structure of the *S. aureus* PI-specific phospholipase C reveals modulation of active site access by a titratable  $\pi$ -cation latched loop. *Biochemistry* **51**, 2579–2587
- Gasteiger, E., Hoogland, C., Gattiker, A., Duvaud, S., Wilkins, M. R., Appel, R. D., Bairoch, A. (2005) in *The Proteomics Protocols Handbook* (Walker, J. M., ed) pp. 571–607, Humana Press, New York
- Feng, J., Wehbi, H., and Roberts, M. F. (2002) Role of tryptophan residues in interfacial binding of phosphatidylinositol-specific phospholipase C. *J. Biol. Chem.* **277**, 19867–19875
- Otwinowski, Z., and Minor, W. (1997) Processing of X-ray diffraction data collected in oscillation mode. *Methods Enzymol.* **276**, 307–326
- Collaborative Computational Project, Number 4 (1994) The CCP4 Suite. Programs for protein crystallography. *Acta Crystallogr. D Biol. Crystallogr.* **50**, 760–763
- McCoy, A. J., Grosse-Kunstleve, R. W., Adams, P. D., Winn, M. D., Storoni, L. C., and Read, R. J. (2007) Phaser crystallographic software. *J. Appl. Crystallogr.* **40**, 658–674
- Emsley, P., and Cowtan, K. (2004) Coot. Model-building tools for molecular graphics. *Acta Crystallogr. D Biol. Crystallogr.* **60**, 2126–2132
- Schüttelkopf, A. W., and van Aalten, D. M. (2004) PRODRG. A tool for high-throughput crystallography of protein-ligand complexes. *Acta Crystallogr. D Biol. Crystallogr.* **60**, 1355–1363
- Krissinel, E., and Henrick, K. (2004) Secondary-structure matching (SSM), a new tool for fast protein structure alignment in three dimensions. *Acta Crystallogr. D Biol. Crystallogr.* **60**, 2256–2268
- Laskowski, R. A., MacArthur, M. W., Moss, D. S., and Thornton, J. M. (1993) PROCHECK. A program to check the stereochemical quality of protein structures. *J. Appl. Crystallogr.* **26**, 283–291
- Yang, H., Guranovic, V., Dutta, S., Feng, Z., Berman, H. M., and Westbrook, J. D. (2004) Automated and accurate deposition of structures solved by x-ray diffraction to the Protein Data Bank. *Acta Crystallogr. D Biol. Crystallogr.* **60**, 1833–1839
- Pu, M., Roberts, M. F., and Gershenson, A. (2009) Fluorescence correlation spectroscopy of phosphatidylinositol-specific phospholipase C monitors the interplay of substrate and activator binding sites. *Biochemistry* **48**, 6835–6845
- Pu, M., Fang, X., Redfield, A. G., Gershenson, A., and Roberts, M. F. (2009) Correlation of vesicle binding and phospholipid dynamics with phospholipase C activity. Insights into phosphatidylcholine activation and surface dilution inhibition. *J. Biol. Chem.* **284**, 16099–16107
- Elson, E. L., and Magde, D. (1974) Fluorescence correlation spectroscopy. I. Conceptual basis and theory. *Biopolymers* **13**, 1–27
- Magde, D., Elson, E. L., and Webb, W. W. (1974) Fluorescence correlation spectroscopy. II. An experimental realization. *Biopolymers* **13**, 29–61
- Thompson, N. L. (1991) in *Topics in Fluorescence Microscopy* (Lakowicz, J., ed) pp. 337–378, Plenum Press, New York
- Rusu, L., Gambhir, A., McLaughlin, S., and Rädler, J. (2004) Fluorescence correlation spectroscopy studies of peptide and protein binding to phospholipid vesicles. *Biophys. J.* **87**, 1044–1053
- Middleton, E. R., and Rhoades, E. (2010) Effects of curvature and composition on  $\alpha$ -synuclein binding to lipid vesicles. *Biophys. J.* **99**, 2279–2288
- Heinz, D. W., Ryan, M., Bullock, T. L., and Griffith, O. H. (1995) Crystal structure of the phosphatidylinositol-specific phospholipase C from *Bacillus cereus* in complex with *myo*-inositol. *EMBO J.* **14**, 3855–3863
- Shi, X., Shao, C., Zhang, X., Zambonelli, C., Redfield, A. G., Head, J. F., Seaton, B. A., and Roberts, M. F. (2009) Modulation of *Bacillus thuringiensis* phosphatidylinositol-specific phospholipase C activity by mutations in the putative dimerization interface. *J. Biol. Chem.* **284**, 15607–15618
- Krissinel, E., and Henrick, K. (2007) Inference of macromolecular assemblies from crystalline state. *J. Mol. Biol.* **372**, 774–797
- Berg, O. G., Yu, B. Z., Apitz-Castro, R. J., and Jain, M. K. (2004) Phosphatidylinositol-specific phospholipase C forms different complexes with monodisperse and micellar phosphatidylcholine. *Biochemistry* **43**, 2080–2090
- Dye, E. S., and Kapral, F. A. (1980) Characterization of a bactericidal system in staphylococcal abscesses. *Infect. Immun.* **30**, 198–203
- Brunger, A. T., Adams, P. D., Clore, G. M., DeLano, W. L., Gros, P., Grosse-Kunstleve, R. W., Jiang, J. S., Kuszewski, J., Nilges, M., Pannu, N. S., Read, R. J., Rice, L. M., Simonson, T., and Warren, G. L. (1998) Crystallography and NMR System. A new software suite for macromolecular structure determination. *Acta Crystallogr. D Biol. Crystallogr.* **54**, 905–921